Metformin Reduces Endogenous Reactive Oxygen Species and Associated DNA Damage

Carolyn Algire[1], Olga Moiseeva[2], Xavier Deschênes-Simard[2], Lilian Amrein[1], Luca Petruccelli[1], Elena Birman[1], Benoit Viollet[3,4,5], Gerardo Ferbeyre[2], and Michael N. Pollak[1]

Abstract

Pharmacoepidemiologic studies provide evidence that use of metformin, a drug commonly prescribed for type II diabetes, is associated with a substantial reduction in cancer risk. Experimental models show that metformin inhibits the growth of certain neoplasms by cell autonomous mechanisms such as activation of AMP kinase with secondary inhibition of protein synthesis or by an indirect mechanism involving reduction in gluconeogenesis leading to a decline in insulin levels and reduced proliferation of insulin-responsive cancers. Here, we show that metformin attenuates paraquat-induced elevations in reactive oxygen species (ROS), and related DNA damage and mutations, but has no effect on similar changes induced by H_20_2, indicating a reduction in endogenous ROS production. Importantly, metformin also inhibited *Ras*-induced ROS production and DNA damage. Our results reveal previously unrecognized inhibitory effects of metformin on ROS production and somatic cell mutation, providing a novel mechanism for the reduction in cancer risk reported to be associated with exposure to this drug.

Introduction

Metformin is a biguanide widely used in the treatment of type II diabetes (1). While details of its mechanism of action remain an active area of research, there is prior evidence that its primary effect is in mitochondria, where it interferes with respiratory complex I and reduces ATP production (2), leading to the activation of AMP kinase (AMPK; ref. 3). In type II diabetes, metformin action in the liver results in inhibition of gluconeogenesis, reducing blood glucose concentration (4, 5), and secondarily reducing the elevated insulin levels characteristic of this condition. Retrospective epidemiologic evidence (e.g., refs. 6–10, reviewed in refs. 11–13) suggests that type II diabetics receiving metformin have substantially lower cancer incidence and mortality than those not receiving this agent, with some reports showing approximately 50% reduction.

Although these epidemiologic data are retrospective and must be considered hypothesis generating rather than conclusive, they have motivated laboratory research to evaluate antineoplastic activities of metformin. Several *in vitro* and *in vivo* experimental systems have shown that metformin reduces growth rates of experimental tumors (e.g., refs. 14–20, reviewed in refs. 12, 21). One class of proposed mechanisms is indirect, and involves the well documented action of metformin on the liver, which results in reduction of the hyperglycemia and hyperinsulinemia characteristic of type II diabetes (14, 15, 18), leading to reduced insulin receptor activation and reduced proliferation of the subset of neoplasms for which hyperinsulinemia provides a growth advantage. There is also evidence for direct actions of metformin on neoplastic cells (16, 17, 19) secondary to various AMPK-dependent antiproliferative effects such as inhibition of mTOR (22), or, for those neoplasms that have impaired ability to survive under conditions of energy stress, cell death related to ATP deficiency (18, 20). However, these mechanisms may not be sufficient to account for the cancer risk reduction reported in pharmacoepidemiologic investigations or observed experimentally. For example, in a tobacco carcinogen-induced lung cancer model, metformin treatment was associated with more than 70% decrease in tumor incidence despite observations that it led to only modest decreases in signaling downstream of the insulin receptor and minimal activation of AMPK (23).

Materials and Methods

Cell lines and culture

AMPKα$^{+/+}$ and AMPKα$^{-/-}$ mouse embryonic fibroblasts (MEF) created by Dr. B. Viollet were provided from the laboratory of Dr. Russell Jones (McGill University, Montreal, QC, Canada). Cells were cultured in 10% FBS Dulbecco's modified Eagle's medium (DMEM; Wisent) with glutamine. Human mammary epithelial cells (HMEC) were obtained from Lonza and grown in 90% mammary epithelial growth medium (MEGM) completed with bovine pituitary extract (BPE), human recombinant epidermal growth factor (hEGF), insulin, hydrocortisone, gentamicin/amphotericin as provided in the MEGM Bullet kit (CC-3150; Lonza), and 10% DMEM (Wisent) supplemented with 10% FBS (Wisent). Identity of cell lines was not reauthenticated as part of the research described here.

Reactive oxygen species quantification by flow cytometry

AMPKα$^{+/+}$ and AMPKα$^{-/-}$ MEFs were plated in 2% FBS DMEM with or without metformin for 48 hours. For analysis, cells were trypsinized, washed in serum-free media, incubated in 10 μmol/L dichlorofluorescein diacetate (DCF-DA; Molecular Probes) with 1 mmol/L H_2O_2 or 500 μmol/L paraquat (1,1′-dimethyl-4,4′-bipyridium dichloride) for 30 minutes, and analyzed by flow cytometry with a FACSCalibur equipped with CellQuest software.

DNA damage immunofluorescence

AMPKα$^{+/+}$, AMPKα$^{-/-}$ MEFs, or primary mammary epithelial cells were plated on glass cover slips in their appropriate medium. Twenty-four hours later, the medium was changed to 2% FBS DMEM and selected groups were treated with 5 mmol/L metformin (Sigma) for 12 hours at which time groups were treated with either 500 μmol/L H_2O_2 or 250 μmol/L paraquat for 36 hours. Cells were washed twice in cold PBS and fixed in 4% paraformaldehyde. Cells were permeabilized with 0.5% Triton X-100 in PBS with 3% BSA and were incubated overnight with a mouse monoclonal anti-phospho-Histone H2AXS134 (1:200; clone JBW301, #05-636, Millipore). Then cells were washed 3 times in PBS with 3% BSA and incubated with a goat anti-mouse secondary antibody (1:1,000; AlexaFluor 488, A-11001, Molecular Probes; Invitrogen) for 1 hour at room temperature. Finally, cells were rinsed 3 times with PBS and were mounted on slides with Vectashield (Vector Laboratories Inc.). Images were captured with an Olympus FV300 confocal laser microscope and were processed with Metamorph and ImageJ.

Immunoblotting

AMPKα$^{+/+}$ and AMPKα$^{-/-}$ fibroblasts were treated with 5 mmol/L metformin (Sigma) for 48 hours followed by treatment of 500 μmol/L H_2O_2, 250 μmol/L paraquat, or 15 μmol/L antimycin for 30 minutes. Primary antibodies against p-ERK, extracellular signal-regulated kinase (ERK) total, AMPK, and β-actin were purchased from Cell Signaling.

SupF forward mutagenesis assay

The SupF plasmid pSP189 and *Escherichia coli* strain MBM7070 were kindly provided by Dr. M. Seidman (National Institute of Aging, NIH, Bethesda, MD). MEFs were trypsinized and washed twice with PBS. Then, 2.5×10E6 cells in 500 μL of PBS were placed in a 4-mm electroporation cuvette and pulsed during 20 ms at 240 V in the presence of 10 μg of plasmid DNA. The plasmid was introduced into MEFs by electroporation. Cells were then plated and treated with 5 mmol/L metformin or vehicle for 15 hours. Then, 25 μmol/L paraquat was added for another 36 hours; plasmids were purified and incubated with the restriction endonuclease *Dpn*I. This endonuclease cleaves plasmids methylated in bacteria focusing the analysis only to plasmid DNA that replicated in mammalian cells. Plasmids were purified again by phenol–chloroform and ethanol precipitation and introduced into MBM7070 *E. coli* strain by electroporation. Bacteria cells were plated into 5-bromo-4-chloro-3-indolyl-β-D-galactopyranoside (X-Gal) indicator plates and blue and white colonies were counted.

Studies of primary fibroblasts with *Ras*-expressing retrovirus

Normal human diploid fibroblasts IMR90 were obtained from American Type Culture Collection and cultured in DMEM (Wisent) supplemented with 10% FBS (Wisent) and 1% penicillin G/streptomycin sulfate (Wisent). Retroviral vectors pBabe and pBabeRasV12 and retroviral-mediated gene transfer were carried out as described in the legend to Fig. 5. Growth curves were obtained from estimations of cell numbers according to a crystal violet retention assay. To measure reactive oxygen species (ROS), cells were incubated with dichlorodihydrofluorescein diacetate (H2DCFDA), dihydroethidium (DHE), or MitoSox from Molecular Probes. Fluorescence was measured by FACS. Immunofluorescence was measured as described earlier.

In vivo paraquat toxicity assay

Male C57BL/6 mice were purchased from Jackson Laboratories at 10 weeks of age. Mice were randomized to receive either metformin (Sigma), 50 mg/kg/d intraperitoneally, for 10 days or PBS of equal volume. On day 11, mice were injected with 50 mg/kg paraquat dichloride (Sigma). To obtain serum, a subset of animals was sacrificed 24 hours after paraquat injection. For survival analysis, viability was recorded every 12 hours after paraquat injection and the survival curve was generated with GraphPad5 software.

8-Isoprostane ELISA

Blood was collected from mice ($n = 10$) 24 hours following paraquat injection by cardiac puncture. Serum was used to measure free 8-isoprostane (Cayman Chemical) following the manufacturer's instructions.

NAD(P)H determination

MEFs were treated with 5 mmol/L metformin for 48 hours, harvested by centrifugation, and resuspended in 10 mmol/L HEPES, pH 7.4, 1.5 mmol/L $MgCl_2$, 10 mmol/L KCl, and 0.05 mmol/L dithiothreitol (DTT). The cells were sonicated and debris pelleted by centrifugation at 4°C. Protein concentration was determined by Bradford assay and NAD(P)H measured by absorbance at 340 nm.

Results and Discussion

Metformin reduces paraquat-induced but not H_2O_2-induced elevations of ROS in an AMPK-independent manner

The primary site of metformin action has been identified as complex I of the respiratory chain, where it inhibits oxidative phosphorylation in a manner distinct from classic complex I inhibitors such as rotenone (2). As complex I is an important source of ROS (24), we studied the influence of metformin on levels of ROS in cells treated with H_2O_2, which acts as an exogenous source of ROS, or paraquat, which stimulates the endogenous production of ROS by complex I (25). Given that several effects of metformin in glucose metabolism and diabetes can be explained by activation of the AMPK (16, 17, 19), we used AMPK$\alpha^{+/+}$ and AMPK$\alpha^{-/-}$ MEFs to evaluate the role of metformin-induced AMPK activation on the observed effects (Fig. 1A). We observed a modest increase in intracellular ROS levels following exposure to metformin in both cell lines (Fig. 1B). As expected, 30-minute exposure to H_2O_2 increased ROS levels, as detected by DCF-DA flow cytometry, and this was not altered when cells were pretreated with metformin for 48 hours, regardless of AMPK expression (Fig. 1B). Exposure to paraquat for 30 minutes increased ROS levels in both cell lines, in keeping with increased endogenous ROS production (Fig. 1B–D). In contrast to the observations with H_2O_2-treated cells, metformin reduced the elevated ROS levels associated with paraquat exposure in both AMPK$\alpha^{+/+}$ and AMPK$\alpha^{-/-}$ MEFs, providing evidence that metformin reduces endogenous ROS levels, in an AMPKα-independent manner.

Metformin blocks paraquat-induced and antimycin-induced, but not H_2O_2-induced, ERK activation

ROS increases ERK signaling (26). We measured p-ERK in AMPK$\alpha^{+/+}$ or AMPK$\alpha^{-/-}$ MEFs following exposure to H_2O_2, paraquat, or antimycin. Antimycin binds to cytochrome c reductase and leads to the formation of large quantities of ROS (27). As shown in Fig. 1E, treatment with paraquat or antimycin for 30 minutes led to a marked increase in p-ERK, consistent with increases in ROS. We observed this effect of H_2O_2, paraquat, and antimycin on ERK phosphorylation in both AMPK$\alpha^{+/+}$ and AMPK$\alpha^{-/-}$ cell lines. In contrast, when cells were pretreated with metformin for 48 hours, we observed an increase in p-ERK following treatment with H_2O_2 exclusively, as 5 mmol/L metformin prevented the increase in ERK phosphorylation following treatment with either paraquat or antimycin in both AMPK$\alpha^{+/+}$ and AMPK$\alpha^{-/-}$ cell lines. The observation that both paraquat and antimycin-induced p-ERK was attenuated by metformin suggests that the drug decreases ROS levels when they are produced by either complex I, the site of action of paraquat (25) or III (the site of action of antimycin; ref. 27). Mechanistically, this is consistent with induction of ROS defenses by metformin, inhibition of ROS production by the mitochondrial electron transport chain, or a direct scavenging action. The fact that metformin itself induces a modest increase in ROS and fails to reduce ROS related to H_2O_2 exposure argues against a scavenger or increased ROS detoxification mechanisms. In aqueous solutions, metformin is a poor scavenger of hydroxyl radicals and does not react with either H_2O_2 or superoxide (28). Hence, the inhibition of ROS production by complex I remains the most plausible mechanism to explain the observed metformin actions. Blocking NADH oxidation by complex I leads to accumulation of NADH (2), a phenomenon that we confirmed in MEFs treated with metformin (Supplementary Fig. S1). Inhibition of complex I reduces entry of electrons to the electron transport chain, and therefore, would reduce ROS production by both complex I and III, consistent with our observations. The modest increase in ROS following metformin exposure suggests NADH-dependent generation of superoxide by the pyruvate dehydrogenase and α-ketoglutarate dehydrogenase complexes (24). These findings provide evidence that metformin acts not as a classic antioxidant but rather as a mitochondrial regulator that decreases ROS production associated with oxidative phosphorylation but not ROS produced by nonmitochondrial sources that are required for normal cell signaling and cellular defenses (29).

Metformin reduces DNA double-strand breaks following paraquat exposure but not following H_2O_2 exposure

Although ROS can damage a variety of cellular components, DNA is a critical target because it can lead to base modifications, abasic sites and double strand breaks, all of which can alter the information content of cells (30). While mitochondrial ROS production would be expected to preferentially damage mitochondrial as compared with nuclear DNA, nuclear DNA mutations are related to ROS levels (31). This does not necessarily require direct action of ROS on nuclear DNA, as it has been shown that nuclear mutation may arise due to direct oxidation of the nucleotide pool by ROS (31). Using γH2AX staining, we quantified DNA double-strand breaks in AMPK$\alpha^{+/+}$ and AMPK$\alpha^{-/-}$ fibroblasts following exposure to H_2O_2 or paraquat, with or without metformin (Fig. 2). Consistent with the observed increases in ROS levels, we observed a significant increase in γH2AX-positive foci in both cell lines following exposure to H_2O_2 and paraquat. Pretreatment with metformin had no effect on H_2O_2-induced DNA damage; however, we observed significant reduction in the number of γH2AX-positive foci following paraquat treatment in the metformin group and,

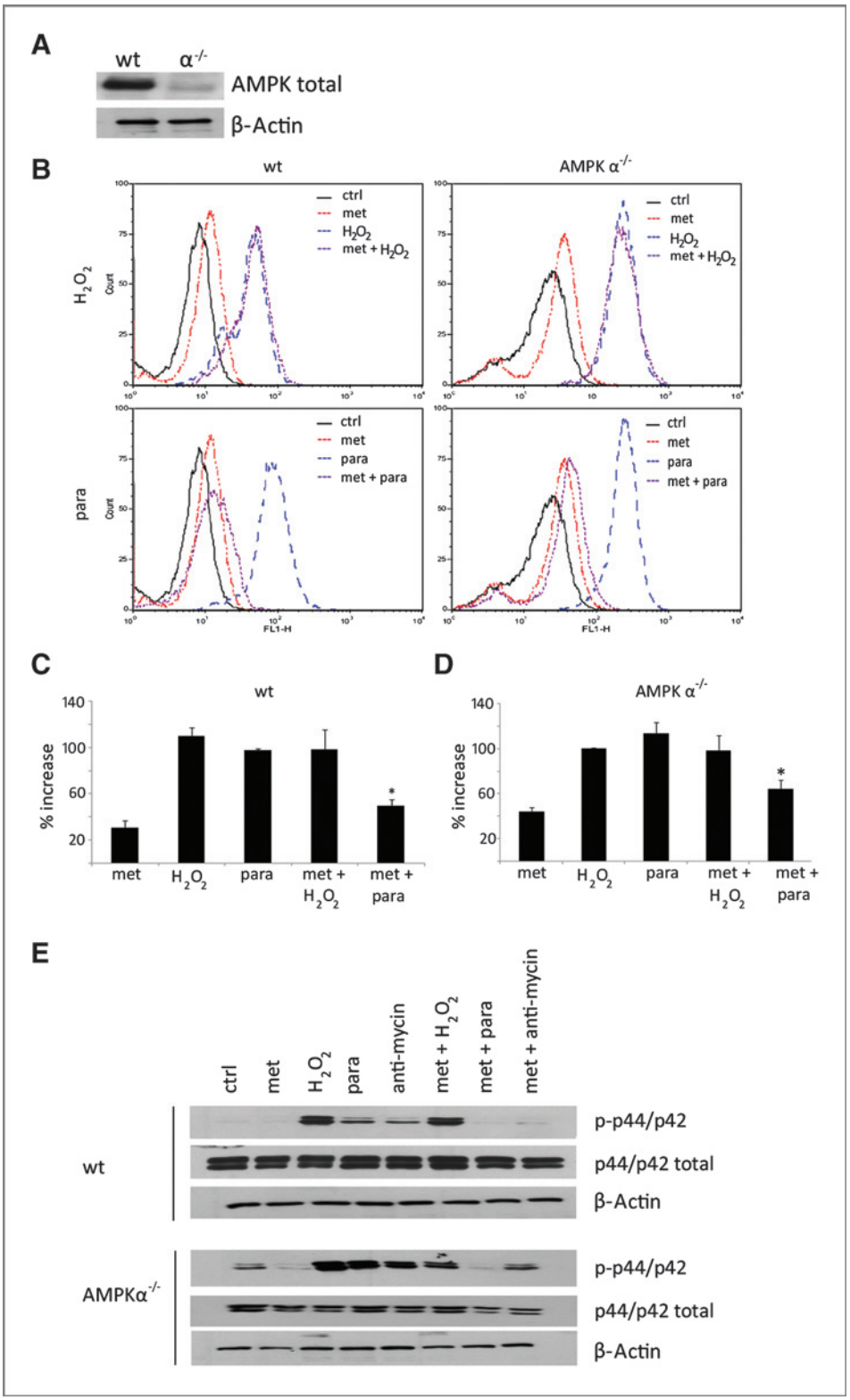

Figure 1. Metformin attenuates the production of ROS and ROS-induced ERK signaling. A, Western blot analysis showing the protein levels of the AMPKα subunit in the AMPKα$^{+/+}$ and AMPKα$^{-/-}$ MEFs. B, AMPKα$^{+/+}$ and AMPKα$^{-/-}$ MEFs were treated with metformin (met), H_2O_2, paraquat (para), or the indicated combinations, and ROS levels were determined by DCF-DA flow cytometry. C and D, quantification of the change in ROS levels seen under the indicated conditions. Error bars represent SEM; the differences between ROS levels under the paraquat alone condition and the paraquat plus metformin conditions were significant ($P < 0.02$). E, Western blot analysis documenting ERK phosphorylation following exposure to H_2O_2, paraquat, or the indicated combinations in both AMPKα$^{+/+}$ and AMPKα$^{-/-}$ mouse embryo fibroblasts. wt, wild-type; ctrl, control.

consistent with our observations in Fig. 1, these results were independent of AMPKα expression. To confirm the generality of our findings obtained in mouse fibroblasts, we repeated this experiment using primary HMEC. Metformin also reduced DNA damage induced by paraquat in these cells (Supplementary Fig. S2).

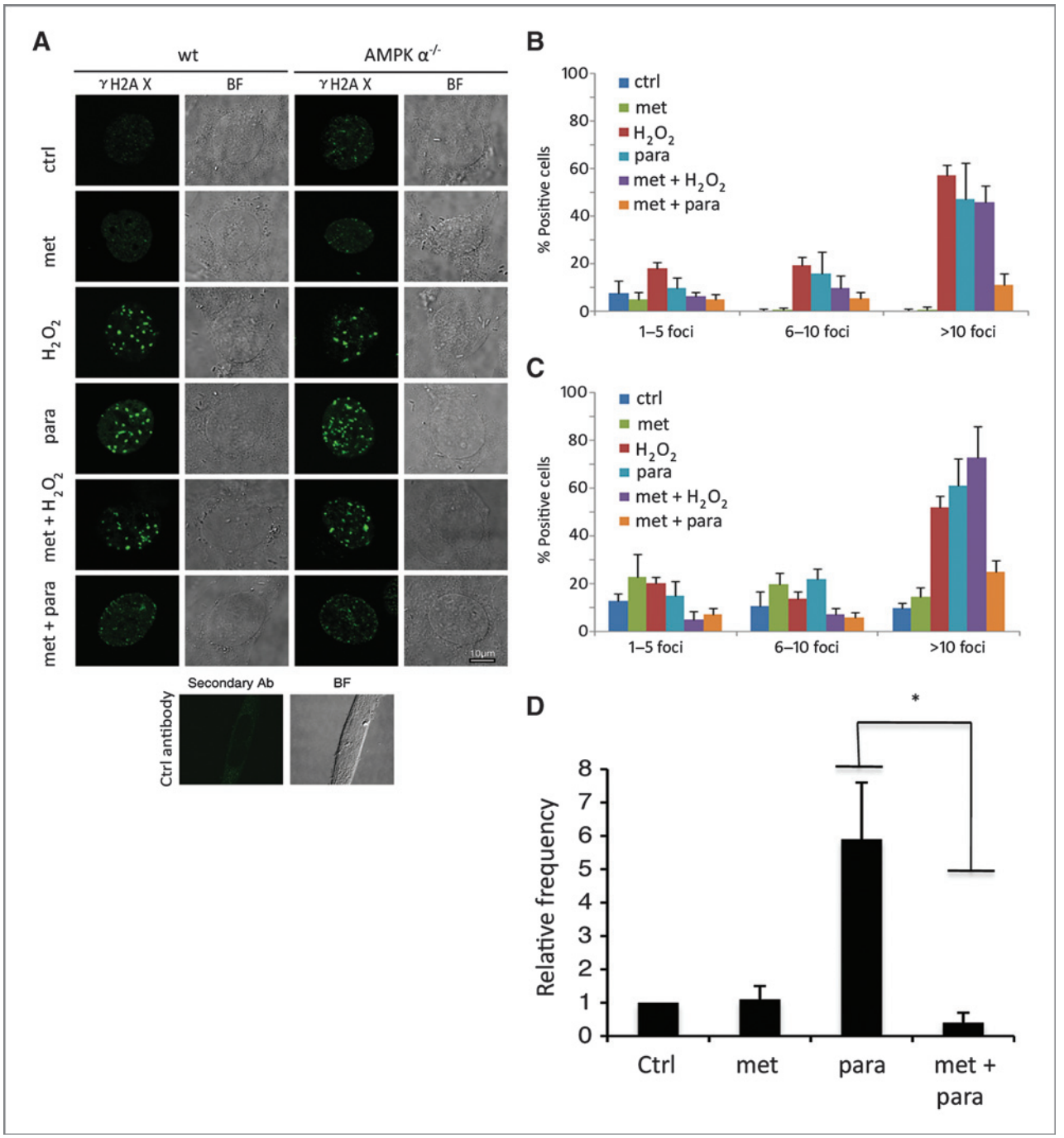

Figure 2. Metformin prevents paraquat-induced, but not H_2O_2-induced, DNA damage in AMPK$\alpha^{+/+}$ and AMPK$\alpha^{-/-}$ MEFs. A, representative images of γH2AX staining showing increased DNA damage, in both cell lines, following treatment with metformin, H_2O_2, paraquat, and the indicated combinations. B and C, bar graphs showing quantification of γH2AX staining data. Error bars represent SEM. For both cell lines, the percentage of cells showing more than 10 foci between the paraquat-only condition and the paraquat plus metformin condition was significant. D, SupF mutagenesis assay in AMPK$\alpha^{+/+}$ MEFs treated under the indicated conditions. The frequency of mutagenesis as reflected by colony count was significantly less under the metformin plus paraquat condition than under the paraquat condition (*, $P = 0.00069$). ctrl, control. BF, Bright field.

Metformin attenuates the paraquat-induced increase in the somatic cell mutation rate as assessed by the SupF forward mutation assay

The relationship between DNA damage and carcinogenesis is complex. The DNA damage response constitutes a barrier for tumor progression (32), and tumors arise when these barriers are inactivated by genetic or epigenetic mechanisms. We considered the possibility that cancer risk reduction by metformin could be attributed at least in part to inhibition of mutagenesis. To evaluate

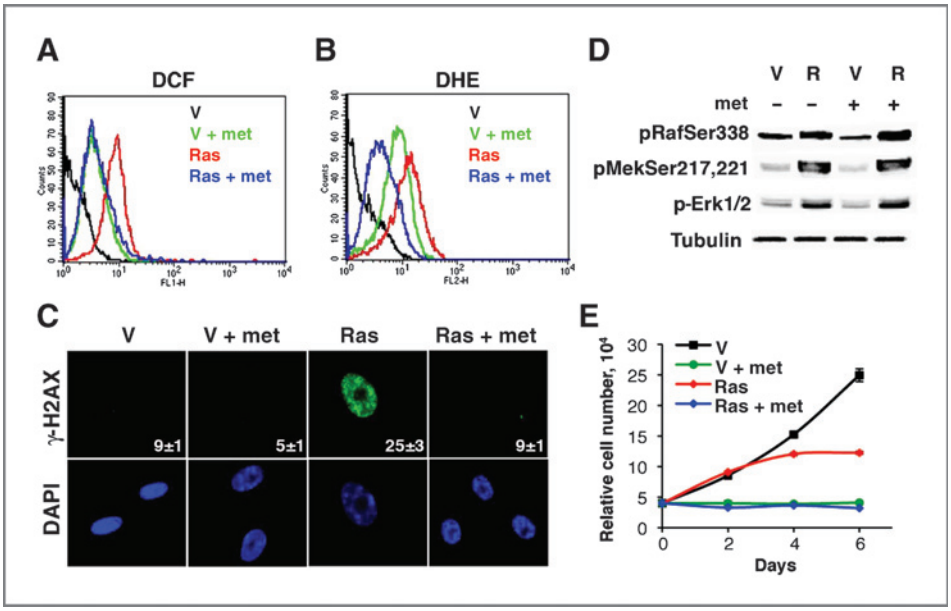

Figure 3. Metformin suppresses the *Ras*-induced increase in ROS and DNA damage in primary human fibroblasts. Primary human fibroblasts (IMR90) were infected with oncogenic *Ras* (R) or a vector control (V), as described in Moiseeva et al. (34). ROS levels were measured in *Ras*-transformed or control fibroblasts in the presence or absence of 5 mmol/L metformin by dicholorodihydrofluorescein diacetate (A) or DHE (B) fluorescence intensity. C, DNA damage foci were estimated by quantifying immunofluorescence for γH2AX. Representative images are shown, and mean number of cells with foci is shown at the bottom right of each panel. D, immunoblots for *Ras* signaling pathway proteins for control or *Ras*-transformed cells, in the presence or absence of 5 mmol/L metformin, showing no effect of metformin on pathway activation. E, growth curves of cells expressing the indicated vectors, in the presence or absence of 5 mmol/L metformin. DAPI, 4′,6-diamidino-2-phenylindole.

this hypothesis, we measured the rate of DNA mutation by the SupF forward mutation assay (33). This method uses a suppressor tRNA (SupF) expression plasmid (pSP189) capable of replicating in mammalian cells. Mutations in the tRNA can be detected in the plasmids purified from mammalian cells using an indicator *E. coli* strain bearing a *lacZ* gene with a stop codon in its open reading frame. We introduced the SupF shuttle vector into MEFs by electroporation and treated with 5 mmol/L metformin for 15 hours. Then, we added paraquat or vehicle for 36 hours and recovered the plasmids. We found that paraquat induced mutations in the SupF tRNA, impairing its ability to suppress the stop codon in the lacZ indictor strain. Metformin prevented the mutagenic effect of paraquat in this assay (Fig. 2D), indicating that its ability to prevent ROS accumulation is associated with a reduction in the mutation rate in mammalian cells.

Metformin attenuates increases in ROS levels and DNA damage foci induced by oncogenic *Ras* expression

Having established that metformin reduces ROS accumulation, DNA damage and mutations in experimental systems involving mitochondrial toxins, we next addressed the question of whether metformin could also prevent these processes when induced by naturally occurring human oncogenes. To investigate this, we introduced oncogenic *Ras* into primary human fibroblasts where it is known to induce ROS production, DNA damage, and cell senescence (34). Consistent with our prior data, 5 mmol/L metformin modestly increased ROS accumulation in the control cells as measured both with superoxide and H_2O_2-sensitive probes (Fig. 3A and B). Metformin attenuated the substantial increase in ROS production observed in *Ras*-expressing cells. Importantly, this was associated with a significant decrease in the number of DNA damage foci (normalized for cell number; Fig. 3C), but had no effect on *Ras* signaling (Fig. 3D) and was associated with reduced proliferation (Fig. 3E). Of note, *Ras*-expressing cells have high levels of superoxide dismutase and catalase despite the fact that they accumulate ROS and associated oxidative DNA damage (34). The ability of metformin to reduce ROS accumulation in these cells is consistent with an effect of reducing ROS formation rather than increasing ROS detoxifying mechanisms, which were previously found to be insufficient to cope with the amounts of ROS produced in *Ras*-expressing cells (34). The finding that metformin attenuates *Ras*-induced ROS production and associated DNA damage is important from the perspective that genome instability is an "enabling characteristic" for neoplasia (35) that can be a consequence of oncogene activation (36). For example, in cases where carcinogens activate *Ras* (37, 38), the induction of further genetic instability and DNA damage is necessary to bypass *Ras*-induced senescence, and this is facilitated by *Ras*-induced ROS production.

Metformin improves survival of mice and attenuates the increase in 8-isoprostanes following paraquat administration

Next, we determined whether metformin influences *in vivo* paraquat toxicity, which is a consequence of increased oxidative stress (39). Twenty mice were randomized to receive paraquat, with or without prior treatment with metformin. Figure 4A shows survival to 120 hours after paraquat injection, at which point all of the mice in the paraquat-only treatment group had died. The mice treated with metformin prior to paraquat administration displayed significantly improved survival. Figure 4B shows the expected increase in levels of free 8-isoprostanes (a marker of oxidative stress *in vivo*; ref. 40) in the serum of mice 24 hours following paraquat injection. This increase was significantly attenuated by metformin, showing that metformin reduces oxidative stress induced by paraquat *in vivo*.

Conclusion

Early pharmacoepidemiologic data suggest a reduction in cancer risk associated with administration of metformin to patients with diabetes. Although these studies are retrospective, and may or may not have implications for subjects without diabetes, the magnitude of the reported protective effect clearly justifies further research. While experimental investigation of the antineoplastic activity of metformin has documented growth inhibitory activity for established cancers, review of the epidemiologic data suggests that the dominant effect of metformin on neoplastic disease may involve reduction in risk rather than improvement in prognosis, as the magnitude of the reported decline in mortality is similar to the magnitude of the decline in incidence. Our finding that sequellae of the previously described (2) mitochondrial actions of metformin include reduced endogenous ROS production, reduced oxidative stress, reduced DNA damage, and reduced mutagenesis in normal somatic cells or their variants expressing activated oncogenes provide a novel mechanism to explain reduced cancer incidence associated with metformin therapy and raise the possibility of novel applications in prevention of cancer and other diseases associated with cellular damage caused by mitochondrial ROS production.

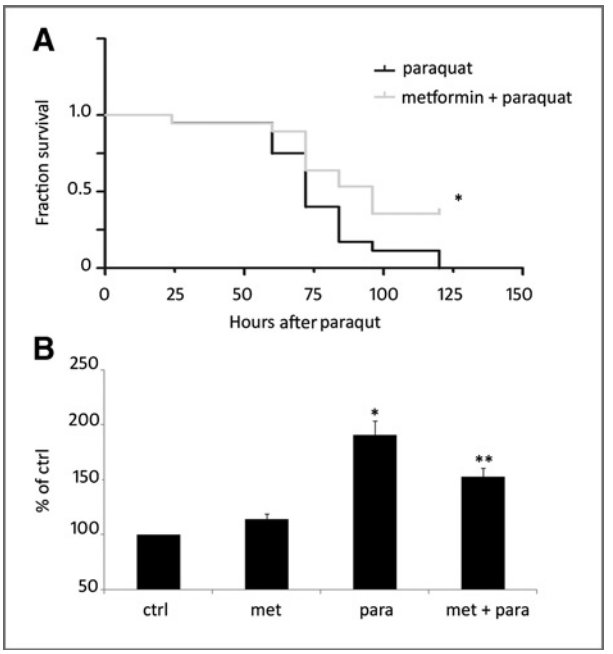

Figure 4. Metformin prolongs survival following administration of paraquat and attenuates the paraquat-induced elevation in serum-free 8-isoprostane level. A, Kaplan–Meier survival curves of mice following a single intraperitoneal injection of 50 mg/kg paraquat, with or without administration of metformin, 50 mg/kg/d intraperitoneally. Metformin administration was associated with improved survival (*, $P < 0.03$), $n = 20$. B, relative serum levels of free 8-isoprostane, a marker of oxidative stress. Bars represent percentage of change in concentration of free 8-isoprostane in the serum of mice 24 hours after paraquat injection under the indicated conditions. Error bars represent SEM. The paraquot-induced increase in levels of this marker relative to untreated animals was significant (*, $P < 0.0001$) as was the difference between the paraquat-exposed condition versus the paraquat plus metformin condition (**, $P < 0.002$), $n = 10$. ctrl, control.

Disclosure of Potential Conflicts of Interest

No potential conflict of interest were disclosed.

The costs of publication of this article were defrayed in part by the payment of page charges. This article must therefore be hereby marked *advertisement* in accordance with 18 U.S.C. Section 1734 solely to indicate this fact.

Received November 23, 2011; revised December 29, 2011; accepted January 13, 2012; published OnlineFirst January 18, 2012.

References

1. Bailey CJ, Turner RC. Metformin. N Engl J Med 1996;334:574–9.
2. Owen MR, Doran E, Halestrap AP. Evidence that metformin exerts its anti-diabetic effects through inhibition of complex 1 of the mitochondrial respiratory chain. Biochem J 2000;348:607–14.
3. Hardie DG. AMP-activated protein kinase: a cellular energy sensor with a key role in metabolic disorders and in cancer. Biochem Soc Trans 2011;39:1–13.
4. Shaw RJ, Lamia KA, Vasquez D, Koo SH, Bardeesy N, Depinho RA, et al. The kinase LKB1 mediates glucose homeostasis in liver and therapeutic effects of metformin. Science 2005;310:1642–6.
5. Foretz M, Hebrard S, Leclerc J, Zarrinpashneh E, Soty M, Mithieux G, et al. Metformin inhibits hepatic gluconeogenesis in mice independently of the LKB1/AMPK pathway via a decrease in hepatic energy state. J Clin Invest 2010;120:2355–69.
6. Libby G, Donnelly LA, Donnan PT, Alessi DR, Morris AD, Evans JM. New users of metformin are at low risk of incident cancer: A cohort study among people with type 2 diabetes. Diabetes Care 2009; 32:1620–5.
7. Bo S, Ciccone G, Rosato R, Villois P, Appendino G, Ghigo E, et al. Cancer mortality reduction and metformin. A retrospective cohort study in type 2 diabetic patients. Diabetes Obes Metab 2012;14:23–9.
8. Bowker SL, Yasui Y, Veugelers P, Johnson JA. Glucose-lowering agents and cancer mortality rates in type 2 diabetes: assessing effects of time-varying exposure. Diabetologia 2010;53:1631–7.

9. Lee MS, Hsu CC, Wahlqvist ML, Tsai HN, Chang YH, Huang YC. Type 2 diabetes increases and metformin reduces total, colorectal, liver and pancreatic cancer incidences in Taiwanese: a representative population prospective cohort study of 800,000 individuals. BMC Cancer 2011;11:20.
10. Bodmer M, Meier C, Krahenbuhl S, Jick SS, Meier CR, Meier CR. Long-term metformin use is associated with decreased risk of breast cancer. Diabetes Care 2010;33:1304–8.
11. Pollak M. Insulin and insulin-like growth factor signalling in neoplasia. Nat Rev Cancer 2008;8:915–28.
12. Pollak M. Metformin and other biguanides in oncology: advancing the research agenda. Cancer Prev Res 2010;3:1060–5.
13. Decensi A, Puntoni M, Goodwin P, Cazzaniga M, Gennari A, Bonanni B, et al. Metformin and cancer risk in diabetic patients: a systematic review and meta-analysis. Cancer Prev Res 2010;3: 1451–61.
14. Algire C, Zakikhani M, Blouin M-J, Shuai JH, Pollak M. Metformin attenuates the stimulatory effect of a high energy diet on *in vivo* H59 carcinoma growth. Endocr Relat Cancer 2008;15:833–9.
15. Algire C, Amrein L, Zakikhani M, Panasci L, Pollak M. Metformin blocks the stimulative effect of a high energy diet on colon carcinoma growth *in vivo* and is associated with reduced expression of fatty acid acid synthase. Endocr Relat Cancer 2010;17:351–60.
16. Zakikhani M, Dowling R, Fantus IG, Sonenberg N, Pollak M. Metformin is an AMP kinase-dependent growth inhibitor for breast cancer cells. Cancer Res 2006;66:10269–73.
17. Dowling RJ, Zakikhani M, Fantus IG, Pollak M, Sonenberg N. Metformin inhibits mammalian target of rapamycin-dependent translation initiation in breast cancer cells. Cancer Res 2007;67:10804–12.
18. Algire C, Amrein L, Bazile M, David S, Zakikhani M, Pollak M. Diet and tumor LKB1 expression interact to determine sensitivity to anti-neoplastic effects of metformin *in vivo*. Oncogene 2011;30: 1174–82.
19. Zakikhani M, Dowling RJ, Sonenberg N, Pollak MN. The effects of adiponectin and metformin on prostate and colon neoplasia involve activation of AMP-activated protein kinase. Cancer Prev Res 2008;1: 369–75.
20. Buzzai M, Jones RG, Amaravadi RK, Lum JJ, DeBerardinis RJ, Zhao F, et al. Systemic treatment with the antidiabetic drug metformin selectively impairs p53-deficient tumor cell growth. Cancer Res 2007;67: 6745–52.
21. Shackelford DB, Shaw RJ. The LKB1-AMPK pathway: metabolism and growth control in tumour suppression. Nat Rev Cancer 2009;9:563–75.
22. Gwinn DM, Shackelford DB, Egan DF, Mihaylova MM, Mery A, Vasquez DS, et al. AMPK phosphorylation of raptor mediates a metabolic checkpoint. Mol Cell 2008;30:214–26.
23. Memmott RM, Mercado JR, Maier CR, Kawabata S, Fox SD, Dennis PA. Metformin prevents tobacco carcinogen-induced lung tumorigenesis. Cancer Prev Res 2010;3:1066–76.
24. Murphy MP. How mitochondria produce reactive oxygen species. Biochem J 2009;417:1–13.
25. Cocheme HM, Murphy MP. Complex I is the major site of mitochondrial superoxide production by paraquat. J Biol Chem 2008;283:1786–98.
26. Sundaresan M, Yu ZX, Ferrans VJ, Irani K, Finkel T. Requirement for generation of H2O2 for platelet-derived growth factor signal transduction. Science 1995;270:296–9.
27. Rieske JS, Lipton SH, Baum H, Silman HI. Factors affecting the binding of antimycin A to complex 3 of the mitochondrial respiratory chain. J Biol Chem 1967;242:4888–96.
28. Khouri H, Collin F, Bonnefont-Rousselot D, Legrand A, Jore D, Gardes-Albert M. Radical-induced oxidation of metformin. Eur J Biochem 2004;271:4745–52.
29. Finkel T. Oxidant signals and oxidative stress. Curr Opin Cell Biol 2003;15:247–54.
30. Cadet J, Douki T, Ravanat JL. Oxidatively generated base damage to cellular DNA. Free Radic Biol Med 2010;49:9–21.
31. Rai P, Young JJ, Burton DG, Giribaldi MG, Onder TT, Weinberg RA. Enhanced elimination of oxidized guanine nucleotides inhibits oncogenic RAS-induced DNA damage and premature senescence. Oncogene 2011;30:1489–96.
32. Halazonetis TD, Gorgoulis VG, Bartek J. An oncogene-induced DNA damage model for cancer development. Science 2008;319:1352–5.
33. Seidman MM, Dixon K, Razzaque A, Zagursky RJ, Berman ML. A shuttle vector plasmid for studying carcinogen-induced point mutations in mammalian cells. Gene 1985;38:233–7.
34. Moiseeva O, Bourdeau V, Roux A, Deschenes-Simard X, Ferbeyre G. Mitochondrial dysfunction contributes to oncogene-induced senescence. Mol Cell Biol 2009;29:4495–507.
35. Hanahan D, Weinberg RA. Hallmarks of cancer: the next generation. Cell 2011;144:646–74.
36. Negrini S, Gorgoulis VG, Halazonetis TD. Genomic instability–an evolving hallmark of cancer. Nat Rev Mol Cell Biol 2010;11:220–8.
37. Wang Y, Zhang Z, Lubet R, You M. Tobacco smoke-induced lung tumorigenesis in mutant A/J mice with alterations in K-ras, p53, or Ink4a/Arf. Oncogene 2005;24:3042–9.
38. Vogt PK. Fortuitous convergences: the beginnings of JUN. Nat Rev Cancer 2002;2:465–9.
39. Bus JS, Gibson JE. Paraquat: model for oxidant-initiated toxicity. Environ Health Perspect 1984;55:37–46.
40. Ferbeyre G, de Stanchina E, Querido E, Baptiste N, Prives C, Lowe SW. PML is induced by oncogenic ras and promotes premature senescence. Genes Dev 2000;14:2015–27.